Published in the Proceedings of the 16th International Aluminum Alloys Conference (ICAA16) 2018
ISBN: 978-1-926872-41-4
by the Canadian Institute of Mining, Metallurgy & Petroleum

MODELING OF ANISOTROPIC BEHAVIOR OF ALUMINUM PROFILE FOR DAMAGE PREDICTION

* F. Andrieux and D. Z. Sun

Fraunhofer Institute for Mechanics of Materials IWM
Freiburg, Germany
*(*Corresponding author: florence.andrieux@iwm.fraunhofer.de)*

ABSTRACT

Extruded aluminum profiles are increasingly used for lightweight vehicle construction. Since fracture strains of aluminum profiles are relatively low, damage modeling is crucial for reliable crash simulation. For aluminum profiles, not only the stress state but also the orientation influenced both the deformation and damage behavior. For the material characterization smooth tensile tests were performed in six orientations, both stress-strain curves and r-values were registered. Moreover notched tensile and shear-tension tests were performed in three directions. Finally punch specimens were tested to investigate biaxial loading. Digital image correlation (DIC) analyses were performed to determine local strain values such as critical values at failure. Numerical investigations were conducted with the strain based damage model GISSMO, which is well suited and widely applied for crash simulation. For a strain based failure model the choice of the deformation model is crucial. Deformation models with increasing complexity were investigated to find the best compromise over all experiments. It was found that there is still a great requirement on development of a material model which describes the orientation dependence of the hardening behavior over all stress states in order to be able to use a strain based failure model reliably.

KEYWORDS

Aluminum profile, Anisotropy, Damage, Failure, FEM simulation, Material modeling, Specimen tests

INTRODUCTION

Weight reduction is an important step for less energy consumption and as a consequence aluminium is increasingly used in automotive parts. An important field of application is the well-established aluminium extrusion which allows the realisation of quite complex shapes of profiles required for an innovative lightweight design with integrated functions. Typical applications are chassis parts, bumpers, crash elements, air bags, etc. Especially the Al–Mg–Si medium strength alloys of the 6000 series can be easily extruded to form complex profiles and prevail for extrusion. Since fracture strains of aluminum profiles are relatively low, damage modeling is crucial for reliable crash simulation. For aluminum profiles not only the influence of the stress state but also the orientation with respect to the extrusion direction have an influence on both the deformation and damage behavior and need to be characterized. The effect of orientation on deformation behavior has been intensively investigated in the last decades and material models haves been proposed (e.g. Barlat & Lian, 1989; Barlat, Lege, & Brem, 1991; Barlat et al., 2003) to describe accurately anisotropic behavior. However it can be noticed that the parameters of anisotropic material models often rely on the yield stress in different directions, which means that the effect of strain hardening is not automatically accounted for. The accuracy of the models at large deformation is not guaranteed and has to be verified. In contrast to deformation models both the characterisation and the modeling of anisotropic damage behavior are not systematically studied. Isotropic failure models based on a critical strain as function of stress triaxiality (ratio of the hydrostatic stress to von Mises equivalent stress) are widely used for crash application (e.g., Bai & Wierzbicki, 2010; Sun, Andrieux & Feucht, 2009; Sun et al., 2013). The mechanisms of failure are manifold and not fully understood; to develop an anisotropic failure model it is mandatory to also have experimental data in different orientations for loading scenarios other than uniaxial tension, e. g. shear, biaxial tension, which implies an extensive experiment plan. This makes the development of failure models more challenging than deformation models for which it is possible to develop a reasonable anisotropic model using the framework of yield function and calibrate the material parameters based on results of tensile tests in different directions. Moreover the development of deformation and failure models are intricate as the variables governing the damage evolution are predicted by the deformation model.

In this work the deformation and failure behavior of an EN AW 6082 (AlMgSi1) in T6 temper is investigated. For this purpose smooth tensile, notched tensile, shear-tension and punch specimens are extracted from profiles and tested under static loading. The tensile specimens are extracted in six directions and the notched and shear specimens in three directions (longitudinal, transverse and diagonal to the extrusion direction). Digital Image Correlation (DIC) analyses are performed to determine local strain values such as critical values at failure. The grain distributions in the extruded profile are evaluated by means of EBSD (Electron Back Scatter Diffraction). Analyses of fracture surfaces on tensile and shear specimens in different directions are performed to investigate failure modes.

Different material models for anisotropic materials are investigated and combined with the strain based failure model GISSMO (Generalized Incremental Stress State dependent damage MOdel) (Neukamm, Feucht, & Haufe 2008) which is implemented in the FE-Code LS-DYNA.

The material model is calibrated based on experimental results. Subsequently, the accuracy of the continuum mechanical approach for simulation of the influence of orientation on damage behavior with respect to numerical effects like element type is discussed.

CHARACTERIZATION OF DEFORMATION AND DAMAGE BEHAVIOR

The experimental characterization is based on tests with specimens extracted from profiles of EN AW 6082 (AlMgSi1) in T6 temper. Both the influence of stress state and orientation on damage development is investigated. In the following the orientation is always given with respect to the extrusion direction and the longitudinal, transverse and diagonal directions are respectively the 0°, 90° and 45° orientations. Figure 1 shows an extraction plan with specimen geometries.

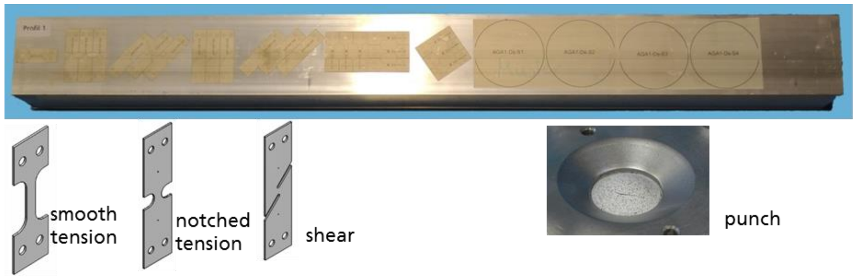

Figure 1. Extraction plan with specimen geometries

Tensile tests on smooth and notched specimens, shear tests on double notched tensile specimens and biaxial tests are performed under static loading. The tensile specimens are extracted in six directions (0°, 15°, 30°, 45°, 60°, 75°, and 90°) and the notched and shear specimens in three directions (0°, 90°, and 45°). The shear specimens are double notched tensile specimens with an angle of 0° between the two notches and the tensile direction, the biaxial specimens are punch specimens.

Tensile Tests

Figure 2 shows the nominal stress vs. strain curves from smooth tensile tests with fracture surface for specimens in 0° and 90°, strain distribution from DIC analysis and technical material values in 0°, 90° and 45° directions. Figure 3 shows the normalized yield stresses (left) and Lankford coefficients (right) as function of the orientation. The orientation dependency of both deformation and failure behavior is obvious. There is no straightforward relation between the yield stresses, Lankford coefficients (r-values) and failure strains and the orientation.

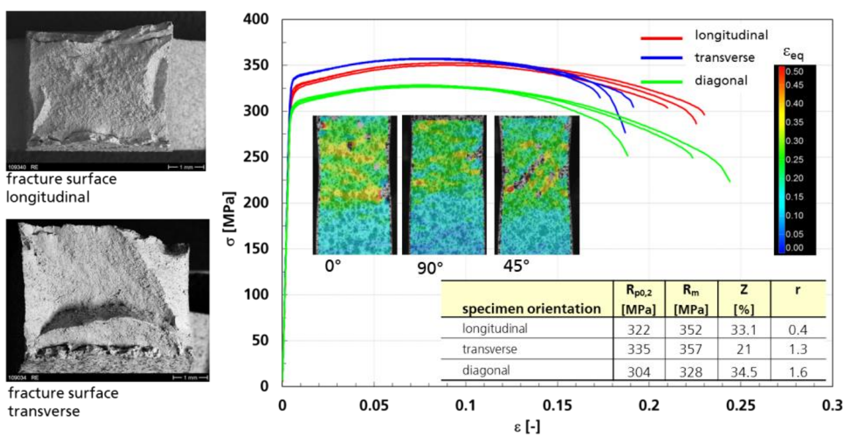

Figure 2. Nominal stress vs. strain curves from tensile tests with fracture surface for specimens in 0° and 90°, strain distribution from DIC analysis and technical material values in 0°, 90° and 45°.

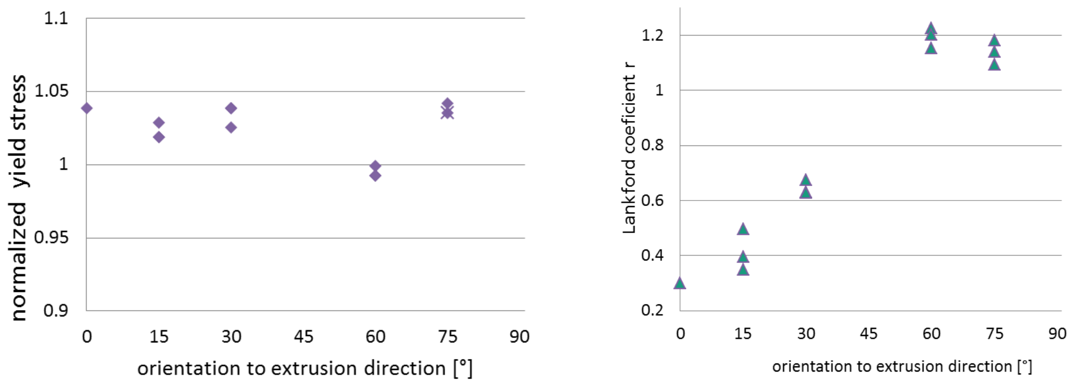

Figure 3. Normalized yield stress (left) and Lankford coefficient (right) as function of the orientation.

Influence of Stress Triaxiality

To investigate the influence of triaxiality on deformation and damage behavior, tests on different specimen types (notched tensile, shear tensile, and biaxial specimens) are performed. The nominal stress vs. strain or displacement curves in 0°, 90° and 45° directions are given in Figure 4 with specimens after tests.

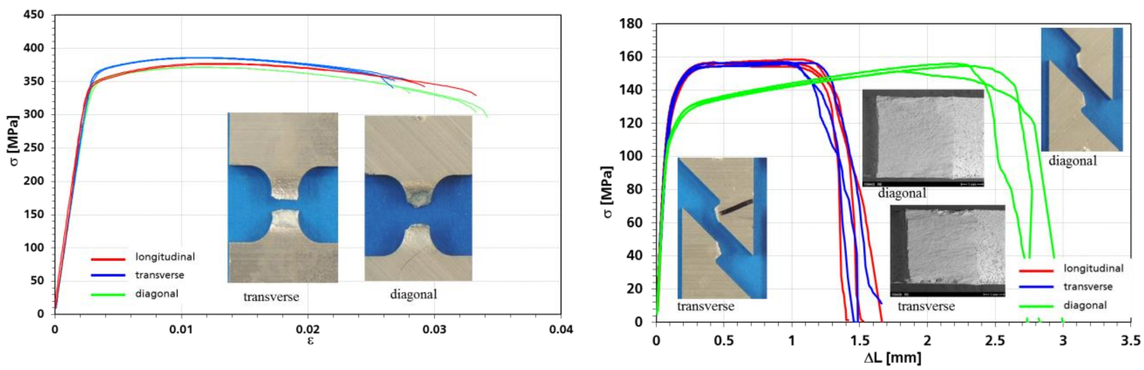

Figure 4. Nominal stress vs. strain or displacement curves from tests on notched (left) and shear (right) specimens in 0°, 90° and 45° directions and specimens after tests and fracture surfaces.

The influence of orientation is affected by the loading situation. At higher stress triaxiality obtained from notched specimens the stress levels in 0°and 45° are similar (Figure 4 left), the stress level in 45° is no longer lower than the one in 0° as obtained in uniaxial case (see Figure 2). This effect can be explained by the high Lankford coefficient in 45° (1.6) indicating a high resistance to thinning flow. Due to the notch influence the thickness deformation is dominant and the high Lankford coefficient leads to a higher axial stress increase than in the other directions (with $r<1$). Due to the large scatter of the material data it is difficult to quantify the effect of high stress triaxiality on orientation dependency of failure strain. A significant effect of stress triaxiality on orientation dependent behavior can be observed at low stress triaxiality obtained from shear tests reported on Figure 4 right. As expected under shear loading the behaviors in 0° and 90° are similar. The behavior in 45° is strongly different concerning yielding, hardening and failure. Moreover the failure always initiates at the notches in each case due to strong strain localization, which is visible on the specimens after test. The specimen geometry needs to be optimized for this material to get failure in the shear region. This indicates a high shear failure strain.

Metallographic Investigations

To complete the experimental characterization EBSD (Electron Backscatter Diffraction) analysis on the initial material and fracture surface analysis by SEM (Scanning Electron Microscope) for the tensile specimens in 0° and 90° and for shear specimens in 90° and 45° are conducted.

EBSD Analysis

The grain distributions in the extruded profile were evaluated by means of EBSD and an example is shown in Figure 5 in which the grain boundaries are determined on the basis of an orientation difference greater than 10 degrees. It is obvious that straps of grains parallel to the extrusion direction were formed which is certainly one reason for the anisotropic behavior. The other reason is the formation of texture in the extruded profile. At the specimen surface a recrystallized coarse grain zone with a size of about 250 µm is formed, in the middle of the specimen a strong texture formation is observed.

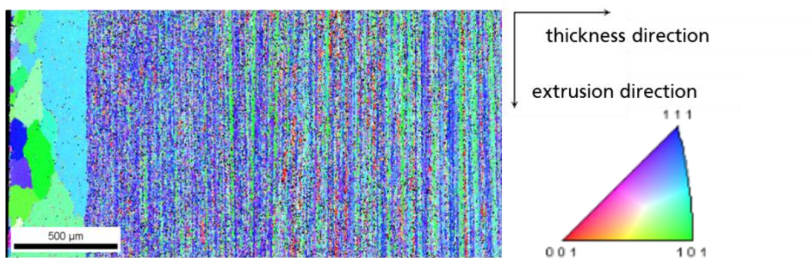

Figure 5. Grain distribution obtained with EBSD.

Fractography

Fracture surface analysis by SEM (Scanning Electron Microscope) for the tensile specimens in 0° and 90° and for shear specimens in 90° and 45° is conducted. Figure 6 shows the fracture surfaces for a tensile specimen in 0° at the surface (a) and in the middle (b) and for a shear specimen in 90° (c). For the tensile specimen an intergranular fracture occurs at the surface (coarse grain zone) while a transgranular fracture with dimples occurs in the middle of the specimen. The fracture surface of the shear specimen in 90° shows a shear fracture with crimped dimples. From the fractographic observations no obvious difference can be pointed out between the fracture surfaces of tensile specimens in 0° and 90° and for shear specimens in 90° and 45°.

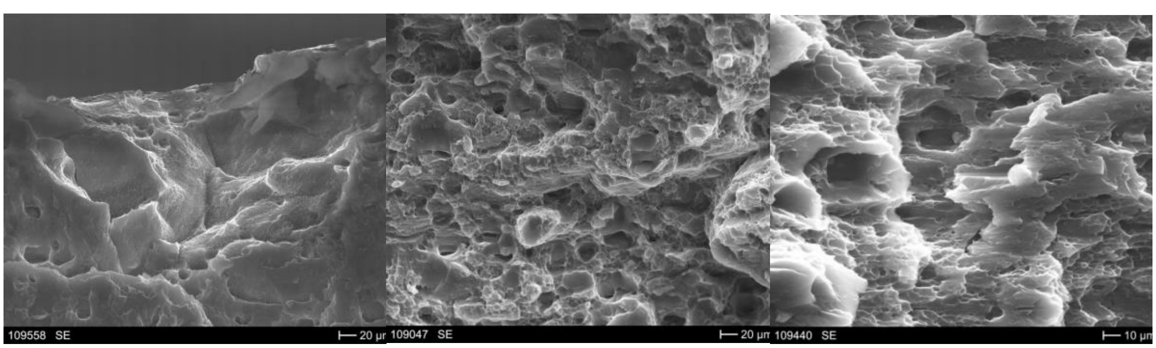

a) tensile specimen 0° border coarse grain zone intergranular fracture	b) tensile specimen 0° middle transgranular dimple fracture	c) shear specimen 90° shear dimples (crimped)

Figure 6. Fracture surfaces a) tensile 0° border b) tensile 0° middle c) shear 90°

CONTINUUM MECHANICAL MODELING

In this work all simulations are performed with the LS-DYNA program.

Material Models

The material models retained in this work are standard models available in LS-DYNA for both deformation and failure.

Deformation

There are several phenomenological plasticity models based on anisotropic yield functions to predict the anisotropic plastic deformation of materials. For almost all anisotropic models available in standard FEM programs the orientation dependent yielding can be described but the hardening law remains the same in all directions. At first the Barlat 3-parameter model (Barlat & Lian, 1989) is investigated. It is widely applied because of the good compromise between simplicity (only three parameters) and accuracy. Moreover, in this work we use an extended version with anisotropic hardening available in the LS-DYNA code. In this extended version an anisotropic hardening is taken into account in a very simplified and empirical way by defining three uniaxial stress-strain curves in 0°, 45° and 90° directions. For this model the three material parameters are internally determined by the code from the three input loading curves.

Better agreement on the yielding can be met with the eight parameter model YLD2000 (Barlat et al., 2003), but in this case the model is only available with isotropic hardening (the same hardening curve for all directions). In the following isotropic hardening is always to be opposed to anisotropic hardening, not to kinematic hardening. The eight material parameters are also internally determined by the code from the input of the yield stresses and r-values in 0°, 45° and 90° as well as the yield stresses under shear and biaxial loadings. Both Barlat models assume plane stress states and are available for shell elements. For large deformation levels which are relevant for crash applications, also by thin structure, the stress states usually deviate from plane stress due to necking or other localisation mechanisms. In order to quantify the numerical effect due to the shell formulation the Barlat 91 model (Barlat, Lege, & Brem, 1991) is also investigated. This model is the extension of Barlat 3 parameter model to general three dimensional stress states; it is only available with isotropic hardening.

Damage

The Barlat 3 parameter and Barlat 91 material models are combined with the strain based failure model GISSMO (Generalized Incremental Stress State dependent damage MOdel). Strain based damage models are widely and successfully used for isotropic materials (e.g., Bai & Wierzbicki, 2010; Sun, Andrieux & Feucht, 2009, Sun et al., 2013). One reason for the large acceptance of strain based models is the evident meaning of the material parameters (critical strain at prescribed triaxiality).

In the flexible GISSMO failure model (Neukamm, Feucht, & Haufe 2008) the failure strain can be defined in a piecewise manner as a linear function of stress triaxiality. To account for loading path changes a cumulative damage variable is defined, its increment is the equivalent plastic strain increment normalised over the critical strain and fracture occurs when the damage reaches a critical value. Although the GISSMO model is initially intended for isotropic behavior it can also be combined to anisotropic material models, as done in this work. In this case the conjugate equivalent strain defined by the deformation model is used for the damage calculation instead of the von Mises equivalent strain. In the following the GISSMO model also when combined with anisotropic deformation behavior is referred as isotropic failure model because the only anisotropic influence comes indirectly from the deformation model and not from the damage model itself.

Figure 7 shows the fracture strains retained for the damage simulations with the Barlat 3 parameter model with the loading paths (equivalent plastic strain vs. stress triaxiality) in the critical elements for the four specimens in all investigated orientations. The symbols represent the values at rupture which are used to determine the failure curve. From this curve it is noticeable that the shear failure strain is low as opposed to the expected high shear strain from experiment results. This low shear failure strain is related to numerical aspects because with 0.5 mm shell elements it is not possible to properly describe the crack propagation from notch to notch. Instead a low failure shear strain has to be introduced to get the final rupture of the ligament between the notches.

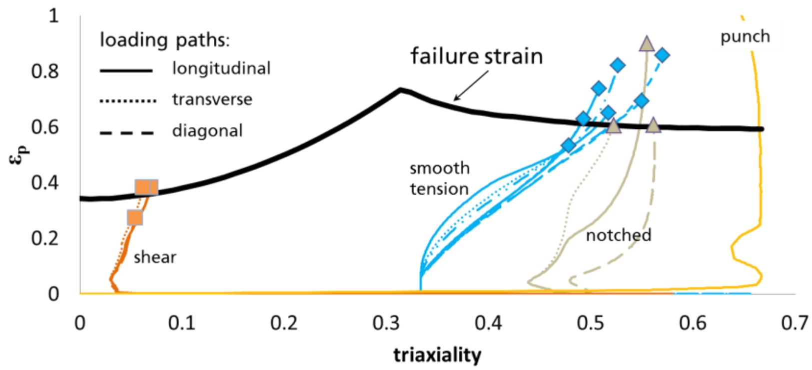

Figure 7. Fracture strain vs. triaxiality with loading paths of critical elements until failure for the simulations with Barlat 3 parameter model.

Modeling of Tests

All the tests are simulated with shell elements using the Barlat 3 parameter model with anisotropic hardening in combination with GISSMO and with the YLD2000 model (without damage). Additional simulations are performed with solid elements using the Barlat 91 model in combination with GISSMO.

Figure 8 shows that the Barlat 3 parameter model can take into account the anisotropic yielding of the material with a good accuracy, especially for the tensile tests at which the parameters are fitted. The big discrepancy between experiment and simulation for the tensile tests in 30° (Figure 8 right) could be partially attributed to material inhomogeneity due to the extraction position in the profile.

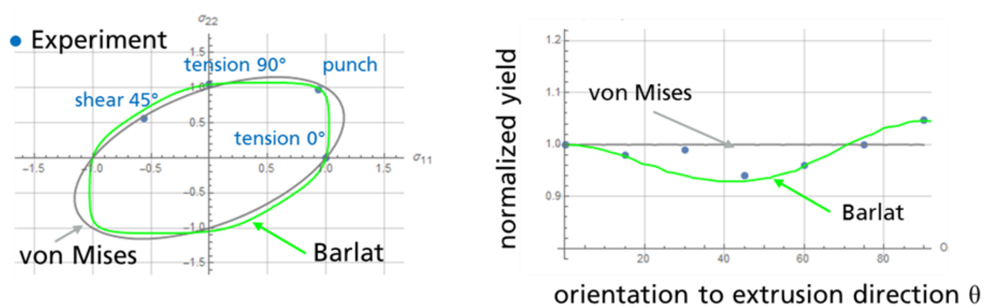

Figure 8. Yield surfaces (left) and normalized yield stresses vs. orientation (right) according to Barlat 3-parameter and von Mises models and in comparison with experiment.

Figure 9 left shows that the Barlat 3 parameter model can predict the tensile tests exactly until the homogeneous strain at the onset of localization; because these three curves are input parameters of the model. As a consequence deformation up to the necking is well predicted. After necking the model is less accurate showing the limitation of the proposed anisotropic hardening model at higher triaxialities. Moreover, because the agreement with experiment remains good, the orientation dependent failure can be well predicted using the isotropic GISSMO model. This is consistent with the fractographic observations showing no obvious difference between the fracture surfaces of tensile specimens in 0° and 90°. Figure 9 right and Figure 8 left show that with the material parameters determined from tensile tests the prediction of shear tests is not accurate for both the yielding and the hardening, as a consequence the failure will not be correctly predicted. As the anisotropic yield function is defined by three parameters and within the anisotropic hardening version they will be determined from the three loading curves in 0°, 45° and 90° it is impossible to adjust the yield function to other stress states like shear.

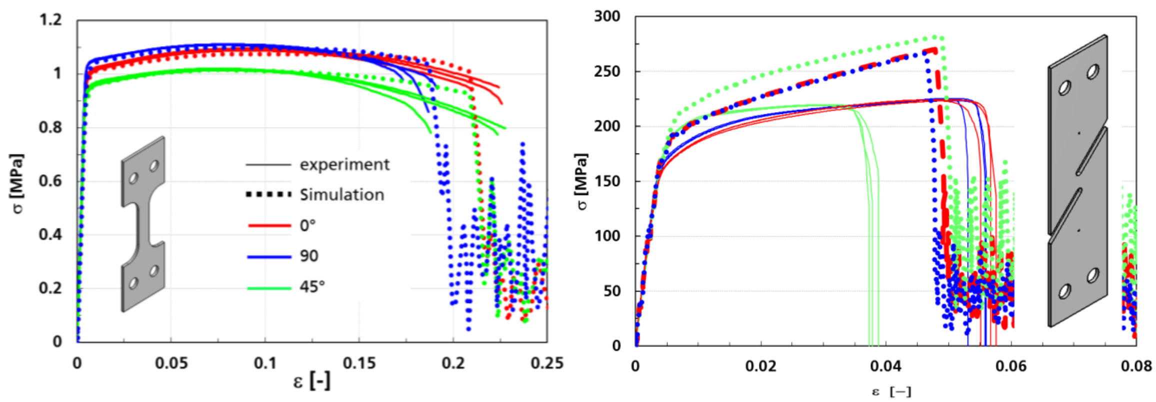

Figure 9. Measured and calculated stress vs. strain curves of tensile (left) and shear (right) tests in 0°, 45° and 90° directions. Simulations with Barlat 3 parameter model in combination with GISSMO.

Figure 10 left shows that the YLD2000 model can predict the yielding in shear tests with a good accuracy. The reason is that the shear tests are used beside the tensile tests in the determination of the eight material parameters, but with increasing deformation the discrepancy with experiment increases. The simulations with the Barlat 1991 model (right) using solid elements give an accurate prediction not only of the yielding in the three directions but also of the hardening at larger strain level. In 0° or 90° the hardening is slightly overestimated which could be due to the material model itself, But this discrepancy remains acceptable. In the parameter determination of the Barlat 91 model the shear tests were also considered, for this reason it was possible to well describe the yielding which was impossible with the Barlat 3 parameter model.

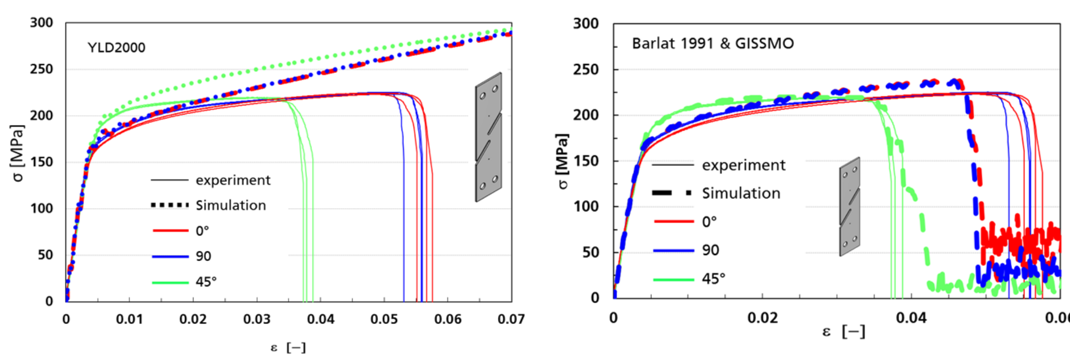

Figure 10. Measured and calculated stress vs. strain curves of shear tests in 0°, 45° and 90° directions. Simulations with YLD2000 (left) and with Barlat 1991 in combination with GISSMO (right).

Interesting is also that in combination with the isotropic GISSMO model it is possible to predict the orientation dependent failure in a good manner. The calculations with the shear failure strain evaluated from the shear test in 45° only slightly underestimates the failure strain in shear tests 0° or 90°. Again this is consistent with the fractographic observations showing no obvious difference between the fracture surfaces of shear specimens in 90° and 45°.

The discrepancy between experiment and simulation obtained with both Barlat 3 parameter and YLD2000 is not only due to the material model but also to the element formulation.

Similar conclusions concerning the deformation behavior can be drawn from the simulations of the notched tensile tests (Figure 11). In this case the YLD2000 model also leads to a quite correct description of the deformation behavior due to the higher flexibility of the yield function with eight parameters. This shows again the complex interaction between element formulation and material model.

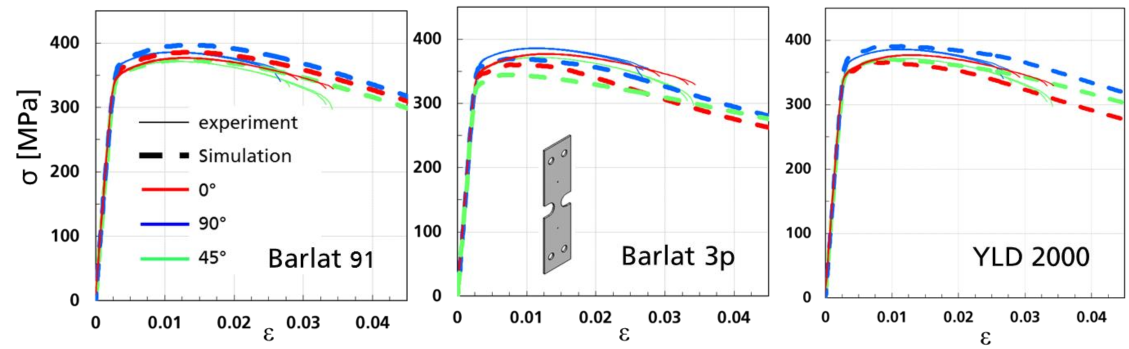

Figure 11. Measured and calculated stress vs. strain curves of notched tensile tests in 0°, 45° and 90° directions. Simulations with Barlat 91 (left), Barlat 3 parameter (middle) and YLD2000 (right).

The limits of the shell formulation can be seen from Figure 12. The equivalent strains obtained with the shell element model Barlat 3 parameter (bottom row of specimens in Figure 12) at a global strain of 0.026 are greater than the values measured from ARAMIS. The 3D model Barlat 91 (top row of specimens in Figure 12) gives an accurate prediction of the strain level on the specimen surface. Moreover the strong deformation gradient over the thickness obtained from the notched tensile test cannot be reproduced using plane stress assumptions.

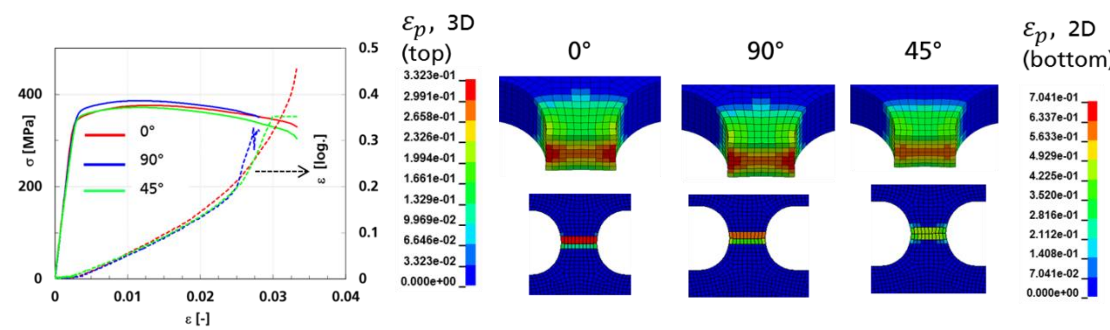

Figure 12. Measured and calculated stress vs. strain curves of notched tensile tests in 0°, 45° and 90° directions with equivalent strain evolution measured from ARAMIS. Distributions of equivalent strain at a global strain of 0.026 with Barlat 91 (top) and Barlat 3p (bottom).

CONCLUSIONS

Extruded aluminum profiles of EN AW 6082-T6 were characterized under different loading situations. There is a strong interaction of stress state and the orientation on the deformation and damage behavior. Anisotropic material models according to Barlat were investigated. The Barlat 3 parameter model gives a good prediction of tensile tests until large strain level for all orientations but this good accuracy is not transferable to other stress states. The YLD2000 model can predict the yielding under all investigated loading cases very well, but at large strain level experiment and simulation are not in very good agreement. For the large strain level considered in this work an important source of discrepancy can be attributed to the element formulation. Shell elements are no more accurate at large deformation also for thin structures because of localisation effects.

Whenever the anisotropic model was able to describe the deformation behavior in all directions over the whole range of deformation it was possible to well describe the failure using an isotropic damage model (e.g., tensile tests with Barlat 3 parameters, shear tests with Barlat91) and also when the global displacements at failure are strongly different as in case of shear loading. This seems to be consistent with fractographic observations showing no distinct failure mechanism between different orientations for the same test type. As for the deformation model it has to be highlighted that the failure strain is related to element formulation and element size.

There is a need to develop a simulation method with an anisotropic deformation model accurate over a large range of deformation and taking into account the element formulation.

REFERENCES

Bai, Y., & Wierzbicki, T. (2010). Application of extended Mohr–Coulomb criterion to ductile fracture. *Int. J. Fract.*, *161*, 1–20.

Barlat, F., & Lian, J. (1989). Plastic behaviour and stretchability of sheet metals. *Int. J. Plast.*, *5*, 51–66.

Barlat, F., Lege, D. J., & Brem, J. C. (1991). A six-component yield function for anisotropic materials. *Int. J. Plast.*, *7*, 693–712.

Barlat, F., Brem, J. C., Yoon, J. W., Chung, K., Dick, R. E., Lege, D. J. & Pourboghrat, F. (2003). Plane stress yield function for aluminum alloy sheets. *Int. J. Plast.*, *19*, 1–23.

Neukamm, F, Feucht, M. & Haufe, A.(2008). Fracture characteristics of three metals subjected to various strains, strain rates, temperatures and pressures, *Proceedings of the 7. LS-DYNA Anwenderforum*, 30 Sept. –1. Oct. 2008, Bamberg, Germany.

Sun, D. Z., Andrieux, F. & Feucht, M. (2009). Damage modelling of a TRIP steel for integrated simulation from deep drawing to crash, *Proceedings of the 7th European LS-DYNA Conf.*, B-III-04.

Sun, D. Z., Ockewitz, A., Falkinger, G., & Andrieux, F. (2013). Characterization and modeling of the deformation and damage behavior of thick-walled aluminum profiles, *Proceedings of the Aluminium Two Thousand 8th World Congress*.